AN EXPLORATORY INVESTIGATION OF VISCOELASTIC NANOINDENTATION ON POLYVINYL ACETATE

By

DILEK CAKIROGLU

Engineering Physics, B.S.
Istanbul Technical University
Istanbul, Turkey
2003

Polymer Science and Technology, M.S.
Istanbul Technical University
Istanbul, Turkey
2006

Submitted to the Faculty of the
Graduate College of the
Oklahoma State University
in partial fulfillment of
the requirements for
the Degree of
MASTER OF SCIENCE
May, 2009

AN EXPLORATORY INVESTIGATION OF

VISCOELASTIC NANOINDENTATION ON

POLYVINYL ACETATE

Thesis Approved:

Dr. Hongbing Lu

Thesis Adviser

Dr. Raman P. Singh

Dr. A. Kaan Kalkan

Dr. A. Gordon Emslie

Dean of the Graduate College

ACKNOWLEDGEMENT

Firstly, I would like to thank you my adviser, Dr. Hongbing Lu, for his guidance, and encouragement throughout this work, and for the opportunity to work in his research group. Also, I would like to thank you Dr. R. P. Singh and Dr. A. K. Kalkan for serving in my committee.

Secondly, I would like to express my thanks to Dr. Jack Houston and Dr. Natan Moore in Sandia National Laboratories for giving a chance to conduct experiments with Interfacial Force Microscopy and sharing their knowledge. Also, I would like to thank to Dr. Nitin Daphalapurkar sharing his knowledge and experiences with me generously throughout this research.

Finally, I would like to thank to my parents for their patience, moral support and encouragement during all stages in the preparation of this thesis.

TABLE OF CONTENTS

Chapter Page

I. INTRODUCTION 7

II. REVIEW OF LITERATURE

2.1 Linear Elastic Indentation 10
2.2 Linear Viscoelastic Indentation 11
2.2 Contact Mechanics Theory 13
2.3 Viscoelastic Behaviors of Polymers 14
2.4 Interfacial Force Microscopy 16

III. METHODLOGY

3.1 Material 19
3.2 Equipments 19
3.2.1 Hysitron Triboindenter 19
3.2.2 Interfacial Force Microscopy (IFM) 21
3.3 Numerical Analysis of Data 21

IV. FINDINGS 23

4.1 Nanaoindentation Measurements with Hysitron Triboindenter 23
4.1.1 Nanoindentation with a Berkovich Indenter 23
4.1.2 Creep Compliance Measurements 27
4.2 Nanaoindentation Measurement with Interfacial Force Microscopy (IFM) 30
4.2.1 Creep Compliance Measurements 33

V. CONCLUSION 36

REFERENCES 38

APPENDIX 41

LIST OF TABLES

Table Page

4.1 Young's Relaxation Modulus at 40 s at different temperatures determined from nanoindentation on Triboindenter 29
4.2 Young's Relaxation Modulus at ~ 3 s at different temperatures determined from nanoindentation on IFM 34

LIST OF FIGURES

Figure Page

2.1 Illustration of JKR method....14
2.1 Schematic structure of Interfacial Force Microscopy....16
3.1 Illustration of heating/cooling stage and thermal control elements....20
4.1 Constant rate loading....24
4.2 Load-displacement curves of PVAc at 24.7 ^{o}C....24
4.3 Experimental and fitted Berkovich nanoindentation load-displacement curves of PVAc at 24.7 ^{o}C....25
4.4 Berkovich nanoindentation load-displacement curves of PVAc at 24.7 ^{o}C and 30 ^{o}C....26
4.5 Experimental and fitted Berkovich nanoindentation curves for PVAc at 42 ^{o}C....26
4.6 All creep compliance curves of PVAc at different temperatures....28
4.7 All shear creep compliance values of PVAc at 40 s at different temperatures....28
4.8 Load-displacement curve of PVAc obtained by IFM....30
4.9 Closed up view of lower portion of load-displacement curve obtained by IFM....31
4.10 JKR fit of load-displacement curve obtained by IFM on PVAc....32
4.11 Fitted and measured IFM nanoindentation load-displacement curves....32
4.12 All shear creep compliance curves of PVAc obtained by IFM at different temperatures....33
4.13 Shear creep compliance values of PVAc at ~3 s at different temperatures....34
A.1 Berkovich nanoindentation on glass at 27 ^{o}C and 31 ^{o}C....42
A.2 Load-displacement curves of PVAc obtained using Triboindenter at 28 ^{o}C....42

A.3 Load-displacement curves of PVAc obtained using Triboindenter at 30 ^{o}C 43
A.4 Load-displacement curves of PVAc obtained using Triboindenter at 32.1 ^{o}C 43
A.5 Load-displacement curves of PVAc obtained using Triboindenter at 34.1 ^{o}C 43
A.6 Load-displacement curves of PVAc obtained using Triboindenter at 36.6 ^{o}C 44
A.7 Load-displacement curves of PVAc obtained using Triboindenter at 38 ^{o}C 44

CHAPTER I

INTRODUCTION

Polymers show different viscoelastic properties that depend on temperature, especially, near the glass transition temperature, T_g. The experimental conditions such as moisture content of the sample have a significant effect on the viscoelastic properties. Polyvinyl acetate (PVAc) is one of the well-known polymeric materials that are so sensitive to moisture. Under isothermal conditions, viscoelastic functions of the polymers can be obtained in either the time or frequency domain. Knauss and Kenner (1980) used a torsiometer shear creep compliance function of PVAc in time domain and Deng and Knauss (1996) obtained the bulk complex creep compliance function in frequency domain. Another technique is nanoindentation to measure the mechanical properties of the materials. Sneddon (1965) provided solution for elastic contact problem. Doerner and Nix (1986) and Oliver and Pharr (1992) developed methods using Sneddon solution (1965) to measure the material properties. These methods use the unloading curve to derive the Young's modulus and hardness. Oliver and Pharr method is mostly used one for monolithic materials and the validity of this method was proved for materials without time-dependence, which contact area does not change with time, by several researchers. However, this method does not work well for viscoelastic contact problems because contact area changes with time. Lee and Radok (1960) analyzed

viscoelastic contact problems and modified elastic solution for viscoelastic contact problems. Lu (2003) developed a method using Lee-Radok approach to measure shear creep compliance function from nanoindentation load-displacement under force controlled loading condition and this method was used by several researchers.

For low indentation load, the effect of adhesive interactions is more dominant and some problems can stem from these interactions during analyzing the data. Johnson-Kendall-Roberts (JKR) (1971) developed a theory to account for the adhesive interactions between tip and linear elastic monolithic material. JKR method was used to get elastic properties of materials from indentation load-displacement data obtained by such as Atomic Force Microscopy (AFM), Interfacial Force Microscopy (IFM).

In this study, nanoindentation load-displacement data of PVAc was obtained at different temperatures ranging from ~20 ^{o}C to 42 ^{o}C using two different equipments, Hysitron Triboindenter and IFM. High load, 600 μN, was applied to a PVAc with Hysitron Triboindenter using Berkovich indenter Low load, 20μN, was applied to a PVAc with IFM using spherical indenter and IFM load-displacement data was analyzed both viscoelastic method and JKR method. Shear creep compliance functions were extracted from each load-displacement data obtained by both equipments.

CHAPTER II

REVIEW OF LITERATURE

Indentation theory for elastic and viscoelastic materials and instrumented nanoindentation using commercial nanoindenter and IFM will be summarized in this chapter.

2.1 Linear Elastic Indentation

For the indentation of linear elastic and isotropic material by a frictionless, rigid and conical indenter, Sneddon (1965) derived equation for relation between indentation load, *P*, and indentation depth, *h*, by

$$h^2 = \frac{\pi(1-\nu)\tan(\alpha)}{4G} P \tag{1}$$

where α is the angle between the half-space and the generator of the conical indenter, υ is Poisson's ratio and *G* is shear modulus.

Similarly, when a frictionless, rigid, spherical indenter of radius *R* is pressed into a linear elastic solid, Hertz (1986) derived equation for relation between indentation load, *P*, and indentation depth, *h*, given as

$$h^{3/2} = \frac{3(1-\nu)}{8G\sqrt{R}} P \tag{2}$$

For indentation to elastic-plastic material, the contact area between indenter and elastic material is needed to find the mechanical properties such as modulus and hardness. Doerner and Nix (1986) found a relationship between contact area and contact stiffness

using the unloading part of load-displacement data. If a spherical indentation is taken as an example, contact stiffness, *S*, is found by using equation (2) as

$$S = \frac{dP}{dh} = \frac{4G\sqrt{R}}{(1-\upsilon)}\sqrt{h} \tag{3}$$

If depth, *h*, is expressed as r_o^2 / R and the area of contact, *A*, is expressed as πr_o^2, the relation between stiffness and contact area is written using Equation (2) as

$$S = \frac{dP}{dh} = \frac{2E\sqrt{A}}{\sqrt{\pi}(1-\upsilon^2)} \tag{4}$$

where *E* is Young's modulus and expressed as $2G(1+\upsilon)$.

Oliver and Pharr (1992) refined Doerner and Nix's approach. In the Oliver-Pharr method, unloading curve is described by a power law relation. They pointed out that Equation (4) can be used even contact area changes continuously and is valid for all indenter geometry. The method developed by Oliver and Pharr is a standard technique to extract the elastic properties of elastic solids in nanoindentation measurements.

2.2 Linear Viscoelastic Indentation

Indentation theory for linear viscoelastic materials was derived from the indentation theory for linear elastic materials. In elastic contact problem, boundary does not change with time, whereas, in the case of viscoelastic contact problem boundary conditions change with time. Therefore, viscoelastic solution can not be simply obtained by replacing the elastic constants with viscoelastic operators. Lee and Radok (1960) provided methods for viscoelastic contact by substituting the hereditary integral operator in place of elastic constants in the elastic solution when the viscoelastic contact area does not decrease with time. For a spherical indenter with radius R, load-displacement relation

is written replacing the P/G in Equation (2) with hereditary integral provided by Lee and Radok (1960) for creep,

$$h^{3/2}(t) = \frac{3(1-\nu)}{8\sqrt{R}} \int_0^t J(t-\xi) \frac{dP(\xi)}{d\xi} d\xi \tag{5}$$

where J is the shear creep compliance function, ξ is a dummy integration variable for time.

In a similar way, for a Berkovich indenter, load-displacement relation is written by modifying Equation (1),

$$h^{2}(t) = \frac{\pi(1-\nu)\tan(\alpha)}{4} \int_0^t J(t-\xi) \frac{dP(\xi)}{d\xi} d\xi \tag{6}$$

In recent years, the early work to the indentation theory for viscoelastic solids was extended by several authors and these indentation theories were applied to the different viscoelastic materials. Lu (2003) devised a method to extract the shear creep compliance function of solid polymers from indentation load-displacement data using Lee and Radok approach in Equations (5) and (6) under controlled loading condition at a constant rate loading. Lu and Gang (2006) devised a method to determine Young's relaxation modulus of solid polymers under indentation depth controlled loading condition. They also developed a method to measure both bulk and shear relaxation functions using an axisymmetric tip and an asymmetric tip. Using the approach developed by Lu, et al. (2003), Sadr (2008) investigated viscoelastic behavior of dental adhesives and Daphalapurkar (2008) investigated viscoelastic behavior of human tympanic membrane. Oyen (2005) measured the spherical indenter tip creep under a constant rate loading and step loading.

Ting (1965), Graham (1965), and Yang (1966) refined Lee and Radok's solution when the viscoelastic contact area changes with time. Kumar and Narasimhan (2004) investigated viscoelastic properties of polymethyl methacrylate (PMMA) using the Ting approach. For a viscoelastic material, decreasing load does not lead necessarily to decreasing displacement. When unloading starts, displacement could keep increasing, after several seconds; displacement starts to decrease and this phoneme is known as "nose" and it is reported by Lu (2003) and Komvopoulos and Zhou (2008). Therefore, Oliver and Pharr method is not applicable to viscoelastic materials. To address this problem Cheng and Cheng (2005) derived a relationship between the initial unloading slope, contact depth and instantaneous relaxation modulus using Ting approach and they claimed that Oliver and Pharr method to find Young's modulus is applicable to indentation for linear viscoelastic solids at sufficiently fast unloading rate. However, no experiment validation was reported.

2.3 Contact Mechanics Theory

Contact mechanics theory was firstly modeled by Hertz (1881) between an elastic spherical body and a rigid sample without taking consideration of the surface forces. Later, this theory was refined by Derjaguin, Mullern and Toporov (1975), known as DMT theory and Johnson, Kendall and Roberts (1971), known as JKR theory. Both DMT and JKR theory account for the adhesive interactions and are applicable to monolithic materials. DMT theory models forces outside of the contact area whereas JKR theory models the contact area between a spherical indenter and an elastic monolithic sample by assuming that short-range forces inside the contact area are

important and long-range forces outside the contact area are negligible. JKR theory is one of the most popular models used today because Hertz and DMT models suggest that loading and unloading are a smooth process and there is no adhesion hysteresis. However, this is not a realistic situation. JKR is more realistic because it allows the adhesion hysteresis during loading and unloading process. JKR model is described by these equations,

$$a = \left(\frac{R|f_c|}{E^*} \right)^{1/3} (1+\sqrt{1+L})^{2/3} \tag{7}$$

$$\delta = \frac{a^2}{R}\left[1 - \frac{2}{3}\left(\frac{a_c}{a}\right)^{3/2} \right] \tag{8}$$

$$f_c = -\frac{3}{2}\pi R\gamma_{12} \tag{9}$$

where a is contact area and a_c is contact area at the maximum adhesive force, seen in Figure 2.1.

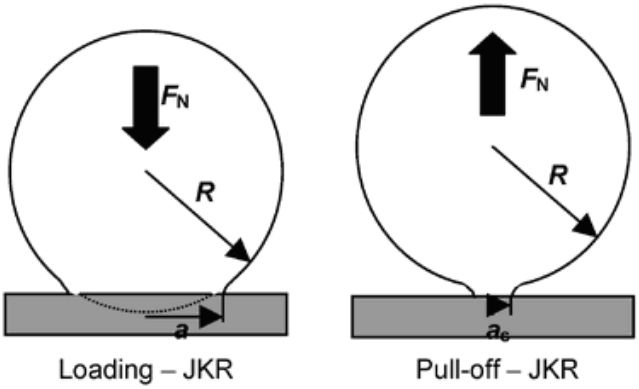

Figure 2.1 Illustration of JKR method (Legget *et al.* 2005)

f_c is maximum adhesive force and called as "pull-off force", L is normalized force and expressed as f/f_c. γ_{12} is adhesion energy and δ is displacement.

2.3 Viscoelastic Behaviors of Polymers

Polymers are in general viscoelastic materials and show different properties at the regions below and above their glass transition temperature, T_g. Above T_g, a polymer acts in a "rubbery" manner in which molecules mobility is high. The modulus in this region is called "rubbery modulus", E_r, and it is low. But below T_g, a polymer acts in a "glassy" manner and modulus is called "glassy modulus", E_g. In the region near T_g, a polymer acts like glassy and rubbery.

Temperature has a strong effect on the mechanical properties of polymers. To determine long-term mechanical properties, short-term experimental results under isothermal conditions, such as creep compliance data, can be shifted horizontally using the time-temperature superposition principle (TTSP) to obtain a master curve. The amount of shifting, called the "shift factors", follows the WLF (Williams, Lander, and Ferry *et al.* 1955)

$$\log[a_T] = \frac{C_1(T - T_{ref})}{C_2 - (T - T_{ref})} \tag{7}$$

where C_1 and C_2 are material constants and they can vary from polymer to polymer and determined experimentally, but generally these values are around $C_1 \sim 8.86$ and $C_2 \sim 101.6$ (Knauss *et al.* 2004). After shifting curves horizontally, we can obtain a master curve which describes the long-term viscoelastic functions. The master curve and shifting factor allow the viscoelastic function to be determined at a given temperature and a given time.

A large number of researchers investigated time-temperature behavior of polymers using different equipments in the time domain. Brinson (1965) investigated creep behavior of epoxy and determined its master curve. Knauss and Kenner (1980)

used a torsiometer to measure shear creep compliance of PVAc at different temperatures and they found equivalence of the effects of moisture and temperature on PVAc if the volumes induced by the two factors are identical. Hinz and his co-workers (2004) investigated Young's modulus of PMMA film using nanoindentation with a scanning force microscope (SFM) at different temperatures. Beake and Gray (2007) determined the creep behavior of polyethylene terephthalate (PET) film with nanoindentation technique at elevated temperatures.

2.4 Interfacial Force Microscopy

IFM was developed at Sandia National Laboratory by Houston and Joyce (1991). IFM is modified form of Atomic Force Microscopy (AFM) except that the probe is mounted to a very tiny "teeter totter", which is supported by torsion bar under capacitor pad, instead of cantilever used in AFM. Schematic structure of IFM is shown in Figure 2.2.

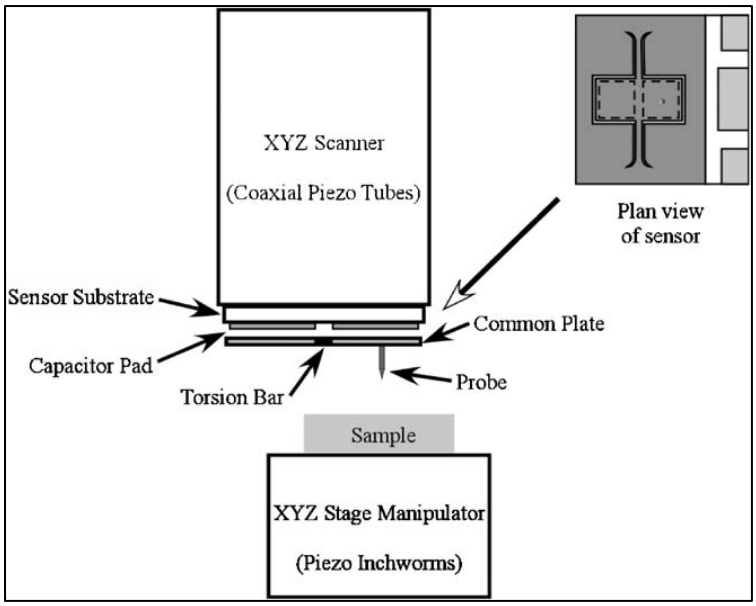

Figure 2.2 Schematic structure of Interfacial Force Microscopy (Liechti *et al*. 2004)

The purpose of the teeter totter is that when the tip is very close to the sample, the attractive force between sample and the tip causes the teeter totter to rotate slightly. This rotation increases the capacitance of one pad and decreases the other one. Feedback system puts the proper voltage to the capacitor pad to rotate it back to zero. Forces are measured based on the voltage used to rotate the capacitor pad back to zero. This feedback mechanism offers superior mechanical stability and the direct measurement of normal and lateral forces (Houston *et al.* 2002). In IFM, force is applied vertically so that the tip position is estimated accurately, whereas in AFM, load is not applied vertically because tip is mounted on the cantilever and bending of the cantilever gives difficulty to estimate the tip position (Norton *et al.* 1998). IFM uses rigid displacement control during indentation, which provides zero load frame compliance (VanLandingham *et al.* 2001). Another advantage of IFM is that jump-to-contact instabilities, which are observed in AFM or other scanning probe microscopy (SPM) systems, are not present in this instrument (Houston and Kiely *et al.* 1998). IFM has capability of measuring adhesive forces produced by attractive and repulsive interactions between sample and the tip (Joyce *et al.* 1992). Also, IFM measures the nanoindentation forces at very small depths under very small load, however commercial nanoindentation system can not give very accurate data at very small depths because of the thermal drift.

IFM made contributions to areas like adhesion, nano-level friction, nanoindentation, and viscoelastic measurements. Houston and Kiely (1998) used IFM to investigate nanomechanical properties of single crystal gold surfaces that has different crystal orientation. Houston and Kim (2001) studied the adhesion, friction and mechanical properties of molecular monolayers self-assembled on gold surfaces with

IFM. Cabibil and his co-workers (2001) measured nanomechanical properties of polysiloxane-oxide thin film. Liechti and his co-workers (2004) examined the nanoindentation of polymeric thin film to extract reduced modulus of film. Study of viscoelastic properties of silly putty with IFM using spherical tip was done by Houston *et al.* (2005). In this research, relaxation function of silly putty under depth controlled load was investigated and Lee and Radok equation was fit to experimental result.

CHAPTER III

METHODOLOGY

3.1 Material

Two different PVAc samples were used in nanoindentation experiments. Sample 1 was a bulk PVAc prepared by molding a PVAc bead between two glass slides in oven at 110 ^{o}C for 1 hour. The oven was turned off with the oven door closed until the sample was cooled down to room temperature. The nominal thickness of bulk PVAc was 0.2 mm and it had a very flat surface. Sample 2 was a PVAc bead, in the form of a circular disk approximately 2 mm in diameter and 1 mm in thickness. Both samples had 170 000 molecular weight (Manufacturer's data). Sample 1 was annealed at temperature 40 ^{o}C in air, and it was cooled down slowly to room temperature by switching off the power of the temperature chamber at a cooling rate of approximately 10 ^{o}C / hr. Sample 2 was dried and stored in nitrogen environment. Sample 1 was stored in a desiccator including desiccant with relative humidity controlled to be less than 50%.

3.2. Equipment

3.2.1 Hysitron Triboindenter

A Hysitron Triboindenter system was used in nanoindentation for the measurements of load-displacement. The system can reach a maximum indentation depth of 5 μm and a maximum load of 10 mN. The displacement resolution is 0.04 nm and the

load resolution is 1nN. A Hysitron temperature controller was used to control the temperature of a sample during experiment. A Peltier thermal element and resistive heater underneath the specimen was used to maintain temperature at the set point. The peltier thermal device allows both heating and cooling from -10 ^{o}C to 200 ^{o}C. Also, the control software package allows a user to change and monitor temperature during experiment. Next to the indenter tip, there is a heating/cooling stage and thermal control elements as illustrated in Figure 3.1.

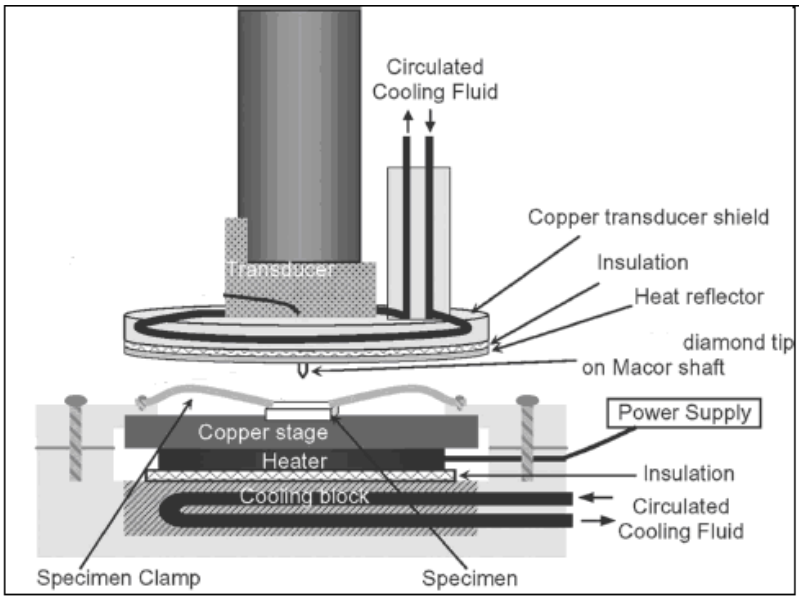

Figure 3.1 Illustration of heating/cooling stage and thermal control elements (Schuh *et al*. 2006)

A diamond Berkovich or spherical tip mounted on a macor shaft, which has low thermal conductivity to protect the tip from elevated temperature, was used. A thermocouple located at the substrate where the sample mounted on was used to monitor the temperature. It was found that it took about 20 minutes to reach the steady state for each different temperature. In this nanoindenter system, tip is not heated so that the tip was brought to make contact with the heated specimen for about fifteen minutes to allow it to reach thermal equilibrium.

3.2.2 Interfacial Force Microscopy (IFM)

An IFM system at Sandia National Laboratories was used in nanoindentation for the measurements load-displacement at small depth up to 16 nm. The IFM system used in this study can reach a maximum load of 50 μN and force resolution was 4 nN. A spherical diamond tip with 10.5 μm radius was used. Dry nitrogen was used to dry the sample. During drying and nanoindentation, a plastic cover was used to insulate the system from environmental effects such moisture. All nanoindentation tests were conducted in air at different temperatures from 20 ^{o}C to 40 ^{o}C. A temperature controller, Model LFI-3751 Wavelength Electronics, was used to control the temperature of stage supporting the sample. After the indenter tip had made contact with the specimen surface, a constant rate displacement was applied and the indentation load and displacement were recorded simultaneously. In each test, nanoindentation did not start until reaching a set temperature to allow the specimen and IFM setup to reach a thermal equilibrium state.

3.3 Numerical Analysis of Data

In this present study, the method developed by Lu et al. (2003) was used to extract the creep compliance function from nanoindentation load-displacement data. In this method, for a spherical indenter under a constant rate loading, v_o, load-displacement relation is given by

$$h^{3/2}(t) = \frac{3(1-\nu)}{8\sqrt{R}}\left[\left(J_o + \sum_{i=1}^{N} J_i\right)P(t) - \sum_{i=1}^{N} J_i v_o \tau_i (1 - e^{-P(t)/(v_o \tau_i)}\right] \qquad (8)$$

where τ_i is retardation time and J_o and J_i are shear creep coefficients, h is the displacement, R is the radius of the indenter, υ is Poisson's ratio and P is the indentation load. A generalized Kelvin model was used to represent shear creep compliance function, $J(t)$.

$$J(t) = J_o + \sum_{i=1}^{N} J_i (1 - e^{-t/\tau_i}) \tag{9}$$

For a Berkovich indenter, load-displacement relation is given by

$$h^2(t) = \frac{\pi(1-\nu)\tan(\alpha)}{4}\left[\left(J_o + \sum_{i=1}^{N} J_i\right)P(t) - \sum_{i=1}^{N} J_i \nu_o \tau_i (1 - e^{-t/\tau_i})\right] \tag{10}$$

Experimental load-displacement data is fitted to Equations (8) and (10) to determine creep compliance numbers and retardation numbers which were then used to find shear creep compliance function using Equation (9). The software was developed using the method described here by Lu et al. (2003) and was named as *'CreepCalculator'*. In this study, CreepCalculator software was used to find creep compliance numbers from nanoindentation data.

Furthermore, contact mechanic analysis was conducted using JKR model for load-displacement data obtained by IFM to extract Young's relaxation modulus.

CHAPTER IV

FINDINGS

4.1 Nanoindentation Measurement with Hysitron Triboindenter

All nanoindentation tests on Hysitron Triboindenter were conducted using a constant-rate nanoindentation load at different temperatures between ~24 ^{o}C and 42 ^{o}C at ~50% relative humidity. The actual temperatures were measured and reported. Only the loading portion in the nanoindentation data was analyzed to determine the creep compliance function.

Temperature increase causes thermal drift and it might give erroneous result, a glass sample was used to calibrate nanoindenter at two different temperatures, 27 ^{o}C and 31 ^{o}C (See Figure A.1). Young's modulus of glass is 70±5 GPa in the literature, nanoindentation results at these two temperatures give 73 GPa.

4.1.1 Nanoindentation with a Berkovich Indenter Tip

In this part of the study, Sample 1, a bulk PVAc, was used. The temperature of the sample was monitored with a thermocouple. A diamond Berkovich indenter tip was used to make nanoindentation to the Sample 1 at a constant loading rate of 0.015 mN/s under 0.6 mN load as shown in Figure 4.1. Nanoindentation was conducted for three

times at different locations of the sample at each different temperature to examine the repeatability of the experiment.

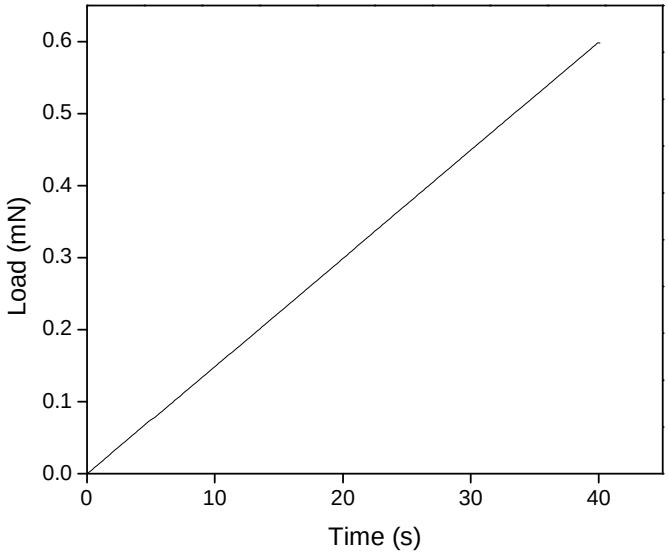

Figure 4.1 Constant rate loading

Figure 4.2 shows several load-displacement curves for 24.7 ^{o}C. The curves are very close to each other, with the maximum difference of 2% at a depth of 350 nm, indicating that results are highly reproducible.

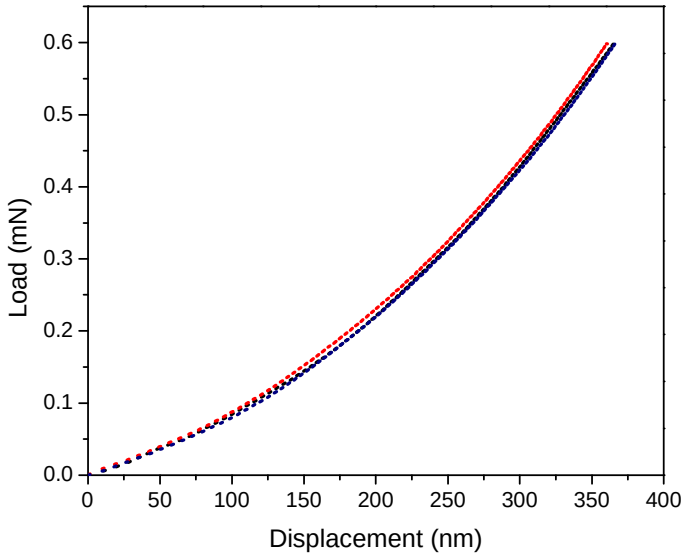

Figure 4.2 Load-displacement curves of PVAc at 24.7 ^{o}C

Figures A.1-A.6 shows the load-displacement curves for 30 ^{o}C, 32.1 ^{o}C, 34.1 ^{o}C, 36.6 ^{o}C, and 38 ^{o}C, respectively. Each load-displacement curve in Figure 4.2 was fitted to Equation (10) to find the best-fit parameters using a constant Poisson's ratio, 0.4, for bulk PVAc sample. The fitted curve is plotted together with the experimental data in Figure 4.3 and the cross-correlation coefficient between two curves is 0.999378, indicating a good correlation between two curves.

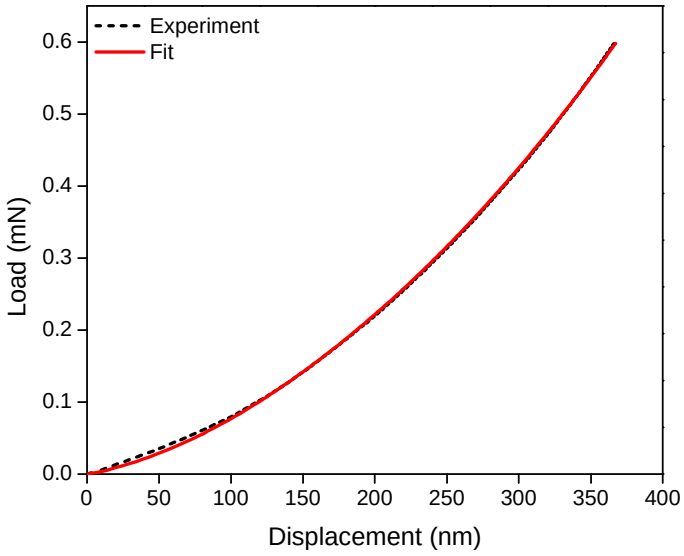

Figure 4.3 Experimental and fitted Berkovich nanoindentation load-displacement curves of PVAc at 24.7 ^{o}C

The same fitting procedure was used at all other temperatures. A very good correlation has been achieved between experimental data and fitted curve at each of these temperatures. Figure 4.4 shows Berkovich nanoindentation load-displacement curves at 24.7 ^{o}C and 30 ^{o}C. Under the same nanoindentation force, depth of nanoindentation increases with increasing temperature due to more pronounced viscoelastic properties of PVAc sample as temperature increases.

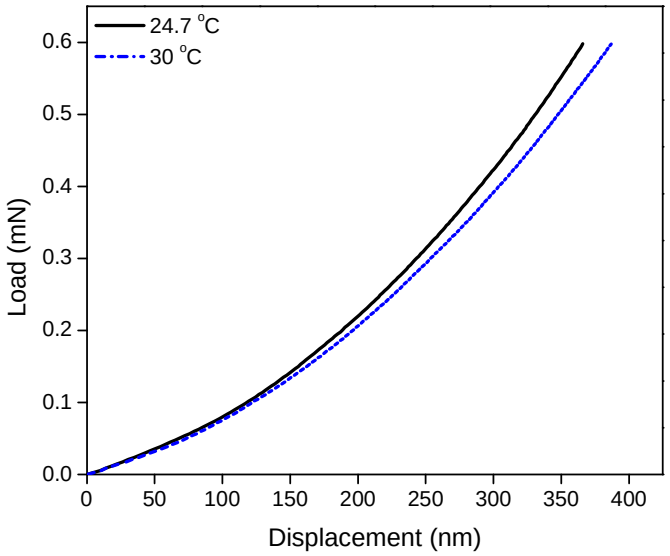

Figure 4.4 Berkovich nanoindentation load-displacement curves of PVAc at 24.7 °C and 30 °C

One nanoindentation was conducted at 42 °C, but at this temperature, PVAc becomes very soft because molecules mobility increases with temperature and curve fitting does not yield good linear viscoelastic parameters to describe the nanoindentation data. Figure 4.5 shows the experimental curve and fitted curve at 42 °C.

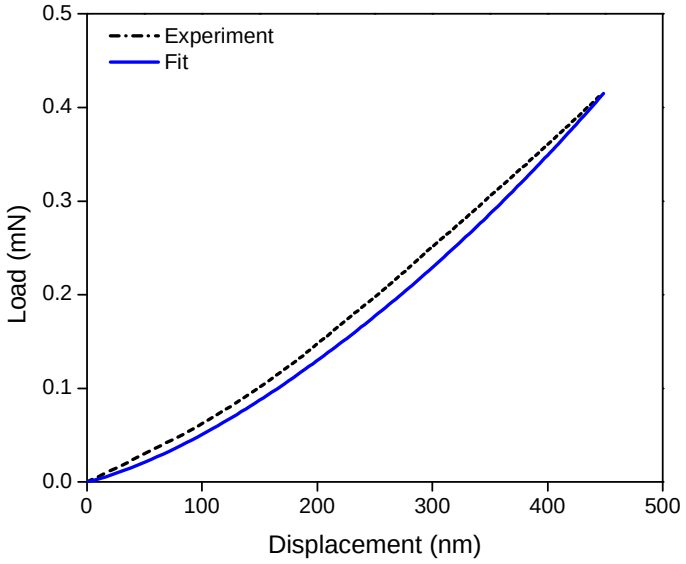

Figure 4.5 Experimental and fitted Berkovich nanoindentation load-displacement curves of PVAc at 42 °C

As seen in the Figure 4.5, at 42 ^{o}C, experimental curve could not be fitted by the method governed by linear viscoelasticity, indicating that the PVAc will most likely behave as a nonlinear viscoelastic material.

4.1.2 Creep Compliance Measurement

In this section, viscoelastic properties of PVAc will be discussed. Shear creep compliance data were obtained for each of the tested temperature using the method explained in section 3.3. Each load-displacement curve obtained at a temperature was analyzed to find the shear creep compliance curve and the average of shear creep compliance curves for each temperature was quoted as the data at that temperature. In the Prony series, eight exponential terms were used in Equation (9). The first retardation time, τ , was 0.001 s and the last retardation time was 1000 s. Each retardation time was 10 times of the previous retardation time. Beginning data was not analyzed because 10 seconds corresponds to nanoindentation displacement less than 50 nm and the data were scattered. Consequently, shear creep compliance was only given after 10 s. Figure 4.6 shows all the shear creep compliance curves obtained at different temperatures. As seen in Figure 4.6, shear creep compliance increases with increasing time and increasing temperature, indicating that PVAc is time and temperature dependent. It is seen that there is a very big gap between curves at 34.1 ^{o}C and 36.6 ^{o}C. The same big gap is seen around 29 ^{o}C in the shear creep compliance data presented on PVAc in the paper by Knauss and Kenner (1980). The big gap is the result of glass transition. If shear creep compliance values at 40 s are plotted, this change can be seen clearly. Figure 4.7 shows the shear creep compliance values at 40 s versus temperature.

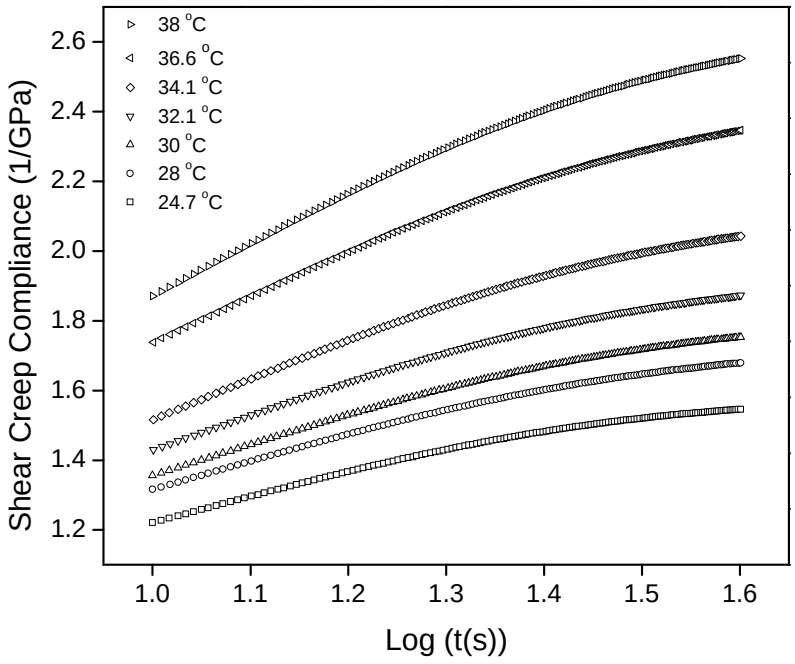

Figure 4.6 All shear creep compliance curves of PVAc at different temperatures

The big gap in the shear creep compliance at around 34 ^{o}C is the indication of glass transition temperature of PVAc.

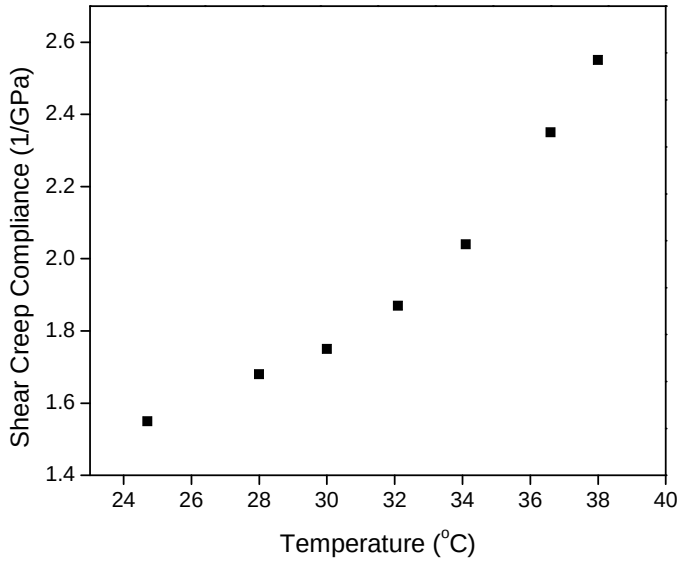

Figure 4.7 All shear creep compliance values of PVAc at 40 s at different temperatures

The reason for different glass transition temperature could be due to difference in materials molecular weights or they could have different manufacturing processes. The molecular weight of the PVAc (353000 M_w) used in Knauss and Kenner's study (1980) is higher than that of the PVAc(170000 M_w) used in this work. The Young's relaxation modulus at 40 s can be estimated from shear creep compliance data using Equation 13 (Daphalapurkar *et al*. 2008),

$$E(long-term) = \frac{2(1+\upsilon)}{J(t \to \infty)} \tag{13}$$

Table 4.1 shows the Young's relaxation modulus at 40 s at several temperatures. Young's relaxation modulus of PVAc at 40 s decreases with increasing temperature; this is the result of viscoelastic properties of polymers.

Table 4.1 Young's relaxation modulus at 40 s at different temperatures determined from nanoindentation on Triboindenter

Temperature (^oC)	Young's Relaxation Modulus (GPa)
24.7	1.81
28	1.67
30	1.60
32.1	1.50
34.1	1.37
36.6	1.19
38	1.1

In this study, horizontal shifting of creep data does not form a master creep curve. The reason might be the drift rate or nonlinear effects of PVAc. In all nanoindentation, drift rate was small, in the order of less than 0.2 nm/s but even small drift rate might create a big error in load-displacement curve and it could result in creep data that does not overlap with each other in long-term.

4.2 Nanoindentation Measurement with Interfacial Force Microscopy (IFM)

In this part, nanoindentation with IFM was conducted on Sample 2, which was a PVAc bead. A diamond spherical tip with 10.5 µm radius was used in nanoindentation. A constant rate loading history at a loading rate of 3.3 µN/s at 20 µN load was applied in nanoindentation. The entire nanoindentation duration was about 6 s. Figure 4.8 shows the typical load-displacement curve obtained at room temperature. Maximum indentation displacement at room temperature was about 16 nm, it is a very small displacement compared with the displacement of more than 300 nm, in nanoindentation on PVAc using the Hysitron Triboindenter.

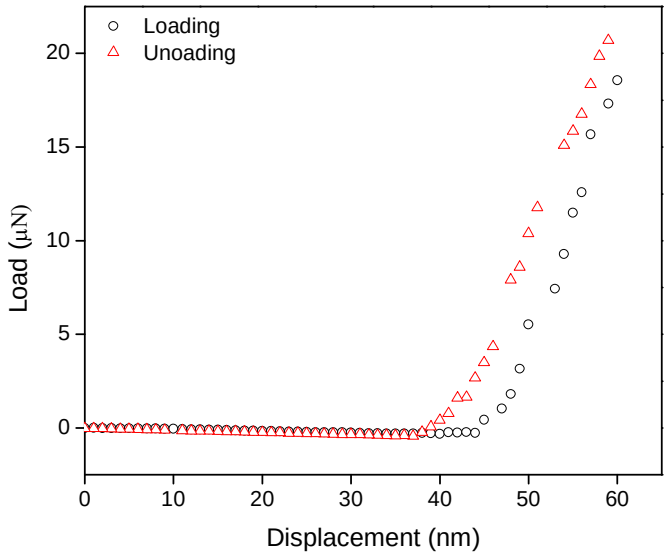

Figure 4.8 Load-displacement curve of PVAc obtained by IFM

As seen in Figure 4.8 there are 4 regions in load-displacement data. From 0 nm to 40 nm, tip approaches the surface of the sample, and then loading starts, from 40 nm to 0 nm, tip withdraws from surface of the sample. Unloading curve does not retrace the loading curve, indicating that the sample was probed viscoleastically. Both curves have small offset, which can be an instrumental artifact due to creep of the piezoscanner (Cabibil and

co-workers *et al.* 2001). Figure 4.9 shows the closed up view of lower portion of the load-displacement curve in Figure 4.8. There is a different force profile very close to the sample surface, indicating that there are strong long-range attractive forces between sample and the indentation tip. These forces have been ascribed to meniscus forces between sample and the tip. Meniscus forces can be result of liquid-like layer on the sample surface or contaminant on the surface of sample or on the tip (Houston and co-workers *et al.* 1992).

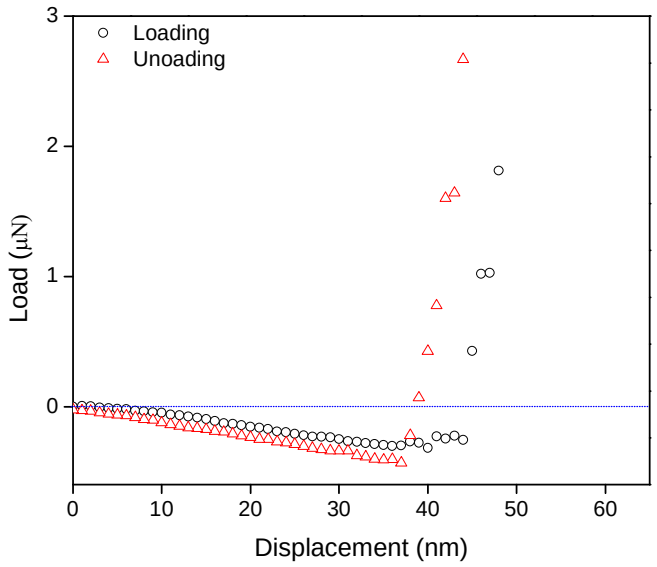

Figure 4.9 Closed up view of lower portion of load-displacement curve obtained with IFM

Contact mechanic analysis was conducted using JKR model. Figure 4.10 shows a JKR fit to the loading curve in one set of data on PVAc. The reduced modulus is 5.3±0.2 GPa obtained from JKR theory is higher than the values obtained by using CreepCalculator and in Knauss and Kenner et al. (1980). This difference might occur because JKR theory is a solution for elastic materials; it does not consider viscoelastic

effects. During approach, loading curve deviates from the elastic model significantly, due to PVAc nonlinear compliance.

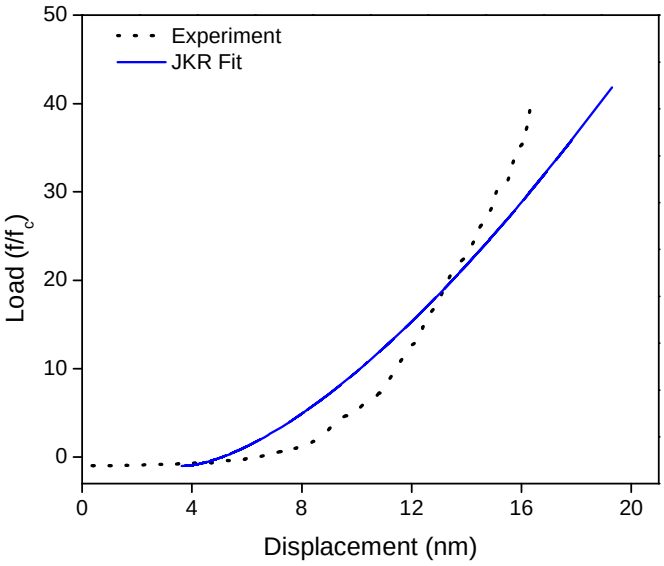

Figure 4.10 JKR fit of IFM nanoindentation data on PVAc

The load-displacement curves obtained from experiment were fit to find the best-fit parameters for the creep compliance using the same method described section 4.2.

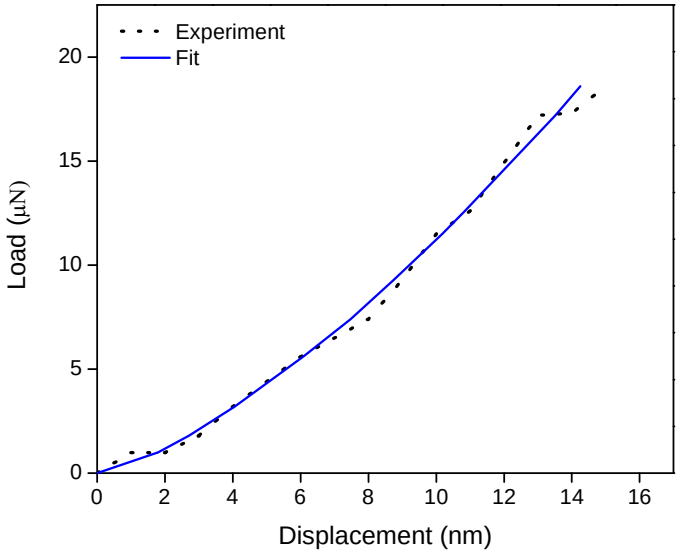

Figure 4.11 Fitted and measured IFM nanoindentation load-displacement curves

Figure 4.11 shows a typical load-displacement curve for PVAc obtained from experiment, and its fitted curve up to 20 μN at room temperature. As seen in Figure 4.11, correlation between two curves is good. The same fitting procedure was used at all temperatures that applied in experiment and a good correlation between experimental data and fitted curve has been achieved. If the two fitting data obtained by JKR theory and viscoelasticity theory on PVAc are compared, the fitting conducted by using viscoelastic theory gives better correlation with experimental data.

4.2.1 Viscoelastic Measurement

In this section, viscoelastic properties of PVAc is discussed. The same values for retardation times, number of terms in Prony series and Poisson's ratio, used in section 4.2.2, were used in creep calculator. The temperature range was from 20 ^{o}C to 40 ^{o}C. Figure 4.12 shows all the shear creep compliance curves at different temperatures. .

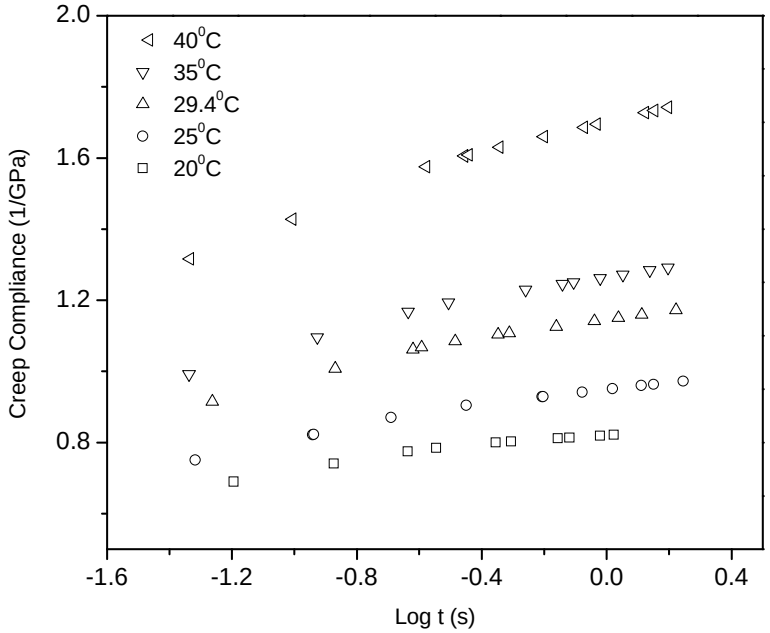

Figure 4.12 Shear creep compliance curves of PVAc at different temperatures obtained using IFM

Loading time was only about 3 s so that only few data point for each temperature can be shown in Figure 4.12. As seen in Figure 4.12, with increasing time and temperature, shear creep compliance of PVAc bead changes, it again shows that PVAc is time-temperature dependent material. The same big gap in shear creep compliance is seen around 34 ^{o}C similar to what was observed in the previous section using the Triboindenter.

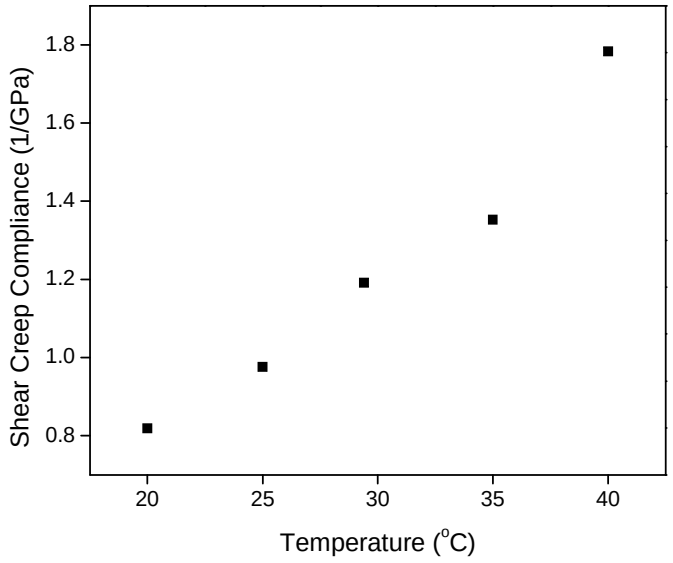

Figure 4.13 Shear creep compliance values of PVAc at ~3 s at different temperatures

The shear creep compliance values at ~3 s versus temperature are shown in Figure 4.13. A big change in shear creep compliance value at ~3 s is observed around 34 ^{o}C.

Table 4.2 Young's relaxation modulus at ~3 s at different temperatures determined from nanoindentation on IFM

Temperature (^{o}C)	Young's Relaxation Modulus (GPa)
20	3.42
25	2.87
29.4	2.35
35	2.07
40	1.57

The Young's relaxation modulus at ~3 s can be determined by inversion of creep function using Equation 11 in section 4.2. Table 4.2 shows the Young's relation modulus at ~3 s. Young's relaxation modulus of PVAc at ~3 s decreases with increasing temperature. However, IFM Young's modulus result is higher than Triboindenter Young's modulus result. This might be the effect of indenter tip or depth of indentation. Because IFM nanoindentation was made with spherical indenter and indentation depth was very small, whereas Triboindenter nanoindentation was made with Berkovich indenter and indentation depth was deeper. Another reason might be the time that the creep data was taken.

CHAPTER V

CONCLUSION

Viscoelastic properties of PVAc samples were investigated using nanoindentation technique at several different temperatures using Hysitron Triboindenter and IFM. Results show that PVAc is time-temperature dependent material. The first set of experimental results was obtained on a Hysitron Triboindenter. Several nanoindentation was conducted between 24 ^{o}C and 42 ^{o}C. Experimental results were highly repeatable and the average of all data at each temperature was analyzed using CreepCalculator to extract the shear creep compliance from experimental load-displacement data. Nanoindentation results obtained on a Triboindenter showed that a PVAc used on this study has glass transition temperature around 34 ^{o}C. The second set of experimental results was obtained using IFM through nanoindentation on a PVAc. Several nanoindentation was conducted between 20 ^{o}C and 40 ^{o}C. The results were analyzed based on JKR theory and viscoelastic theory to find viscoelastic functions of a PVAc. Shear creep compliance of PVAc was determined by using CreepCalculator. Young's modulus determined by JKR theory showed the higher value than the value obtained by using viscoelastic theory. Also, nanoindentation results using IFM showed that a PVAc has glass transition temperature around 34 ^{o}C. Both experimental results are confirmed

each other. Also, master creep data could not be formed using Triboindenter; it shows that even small drift rate created by machines results in big error in creep data.

REFERENCES

Knauss, G.W., Kenner, H.V., 'On the hygrothermomechanical characterization of Polyvinyl Acetate', *J. Applied Physics,* **51**(10), 1980, 5131-5136

Deng, H.T., Knauss, G.W., 'The temperature and frequency dependence of the bulk compliance of Poly(Vinyl Acetate)', *Mechanics of Time-Dependent Materials,* **1**,1996, 33-49.

Lee, E.H., Radok, J.R.M., 'The contact problem for viscoelastic bodies', *J. Applied Mech.,* **27**, 1960, 438-444

Lu, H., Wang, B., Ma, J., Huang, G., Viswanathan, H., 'Measurement of creep compliance of solid polymers by nanoindentation', *Mech. Time-Dependent Material*, **7**, 2003, 189-207.

Johnson, L., Kendall, K., Roberts, D.A., 'Surface energy and the contact of the elastic solids', *Proc. R. Soc. London A324*, **301**, 1971

Sneddon, I.N., 'The relation between load and axisymmetric boussinesq problem for a punch of arbitrary profile', *International Journal of Engineering and Science*, **3**, 1965, 47-57

Hertz, H., 'Uber die Beruhrung fester elastischer Korper', *Journal fur die Reine und Angewandte Mathematik,* **92**, 1881, 156-171

Doerner, F.M., Nix, D.W., 'A method for interpreting the data from depth-sensing indentation instruments', *J. Material Science*, **1**, 1986, 601-609

Oliver, C.W., Pharr, M.G., 'An improved technique for determining hardness and elastic modulus using load and displacement sensing indentation experiments', *J. Material Research,* **7**, 1992, 1564-1583

Huang, G., Lu, H., 'Measurement of Young's relaxation modulus using nanoindentation', *Mech. Time-Dependent Mater*, **10**, 2006, 229-243

Huang, G., Lu, H., 'Measurement of two independent viscoelastic functions by nanoindentation', *Experimental Mechanics*, **47**, 2007, 87-98.

Sadr, A., Shimada, Y., Lu, H., Tagami, J. 'The viscoelastic behavior of dental adhesives: A nanoindentation study', *Dental Materials*, **24(11),** 2008, 1534-1538

Huang, G., Daphalapurkar, N., Gan, Z.R., Lu, H., 'A method for measuring linearly viscoelastic properties of human tympanic membrane using nanoindentation', *Journal of Biomechanical Engineering – Transactions of ASME*, **130**, 2008

Oyen, L.M., 'Spherical indentation creep following ramp loading', *J. Material Research*, **20**, 2005, 2094-2100

Ting, T.C.T., The contact stresses between a rigid indenter and a viscoelastic half-space', *J. Applied Mechanics*, **33**, 1966, 845-854

Graham, G.A.C., 'The contact problem in the linear theory of viscoelasticity', *International J. of Engineering Science*, **3**, 1965

Yang, W.H., 'The contact problem for viscoelastic bodies', *J. Applied Mechanics*, **33**, 1966

Kumar, R.V.M., Narasimhan, R., 'Analysis of spherical indentation of linear viscoelastic materials', *Current Science*, **87**, 2004, 1088-1095

Zhou, J., Komvopoulos, K., 'Surface and interface viscoelastic behaviors of thin polymer films investigated by nanoindentation', *J. Applied Mechanics*, **100**, 2006,1-8

Cheng, T.Y., Cheng, M.C., 'Relationship between contact stiffness, contact depth, and mechanical properties for indentation in linear viscoelastic solids using axisymmetric indenters', *Struct. Control Health Monit.*, **13**, 2006, 561-569

Williams, L.M., Landel, F.R., Ferry, D.J., 'The temperature dependence of relaxation mechanisms in amorphous polymers and other glass-forming liquids', *J. American Chem. Society*, **77**, 1955, 3701-3707

Knauss, G.W., 'Viscoelastic material characterization relative to constitutive and failure response of an elastomer', *Final report to the office of naval research*, 2004

Brinson, F.H., Brinson, C.L., *'Polymer Engineering Science and Viscoelasticity'*, first ed., Springer Press, 2008

Hinz, M., Kleiner, A., Hild, S., Marti, O., Durig, U., Gotsmann, B., Drechsler, U., Albrecht, R.T., Vettiger, P., 'Temperature dependent nanoindentation of thin polymer films with the scanning force microscope', *European Poly. J.*, **40**, 2004, 957-964

Gray, A., Beake, D.B., 'Elevated temperature nanoindentation and viscoelastic behavior of thin poly(ethylene terephthalate) films', *J. Nanoscience and Nanotech.*, **7**, 2007, 2530-2533

Joyce, A.S., Houston, J., 'A new force sensor incorporating force-feedback control for interfacial force microscopy', *Rev. Sci. Instrum.*, **62**, 1991, 710

Houston, J., Kim, H., 'Adhesion, friction, and mechanical properties of functionalized alkanethiol self-assembled monolayers', *Accounts of Chemical Research*, **35**, 2002, 547-553

Warren, L.O., Graham, F.J., Norton, R.P., 'Tapping mode imaging with an interfacial force microscope', *Rev. Sci. Instrum.*, **68**, 1997, 4124-4131

VanLandingham, R.M., Villarrubia, S.J., Guthrie, F.W., Meyers, F.G., 'Nanoindentation of polymers: an Overview', *Macromolecule Symp.*, **167**, 2001, 15-43

Joyce, A.S., Thomas, C.R., Houston, E.J., Michalske, A.T., Crooks, M.R., 'Mechanical relaxation of organic monolayer films measured by Force Microscopy', *Physical Rev. Letters*, **68**, 1992, 2790-2793

Kiely, D.J., Houston, E.J., 'Nanomechanical properties of Au (111), (001), and (110) surfaces, *Physical Rev. B*, **57**, 1998, 12588-12594

Houston, J., 'A local-probe analysis of the rheology of a solid-liquid', *Journal of Polymer Science: Part B: Polymer Physics*, **43**, 2005, 2993-2999

Cabibil, H., Celio, H., Lazona, J., White, M.J., 'Nanomechanical properties of poly siloxane-oxide interphases measured by interfacial force microscopy', *Langmuir*, **17**, 2001, 2160-2166

Wang, M., Liechti, M., White, M.J., Winter, M.R., 'Nanoindentation of polymeric thin films with an interfacial force microscopy', *Journal of Mechanics and Physics of Solids*, **52**, 2004, 2329-2354

Schuh, A.C., Packard, E.C., Lund, C.A., 'Nanoindentation and contact-mode imaging at high temperatures', *J. Material Research*, **21**(3), 2006, 725-736

Daphalapurkar, N., Dai, C., Gan, Z.R., Lu, H., 'Characterization of the linearly viscoelastic behavior of human tympanic membrane by nanoindentation', *Journal of the Mechanical Behavior of Biomedical Materials*, **2**, 2008, 82-92

Legget, J.G., Brewer, J.N., Chong, L.S.K., 'Friction force microscopy: towards quantitative analysis of molecular organization with nanometer spatial resolution', *Phys. Chem. Chem. Physics*, **7**, 2005, 1107-1120

APPENDIX

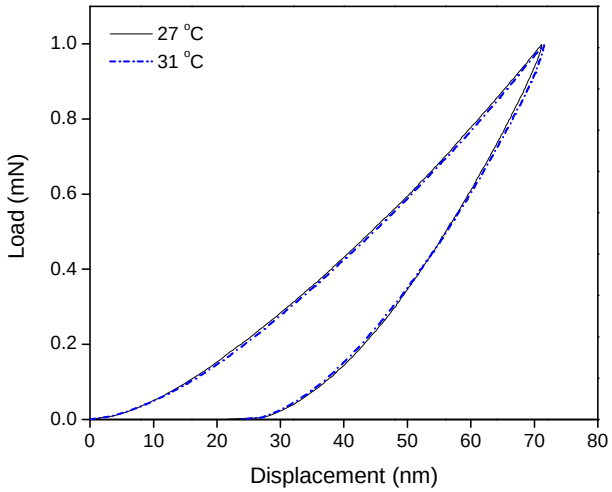

A.1 Berkovich nanoindentation on glass at 27 °C and 31 °C

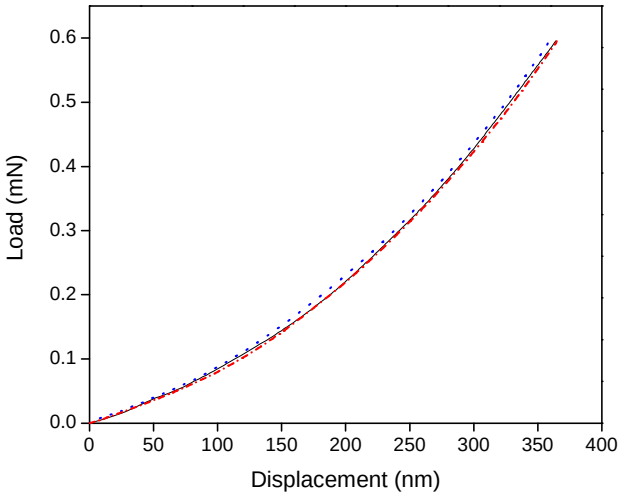

A.2 Load-displacement curves of PVAc obtained using Triboindenter at 28 °C

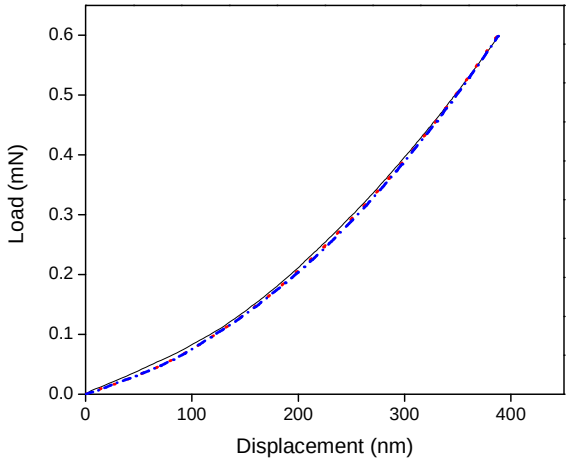

A.3 Load-displacement curves of PVAc obtained using Triboindenter at 30 ^{o}C

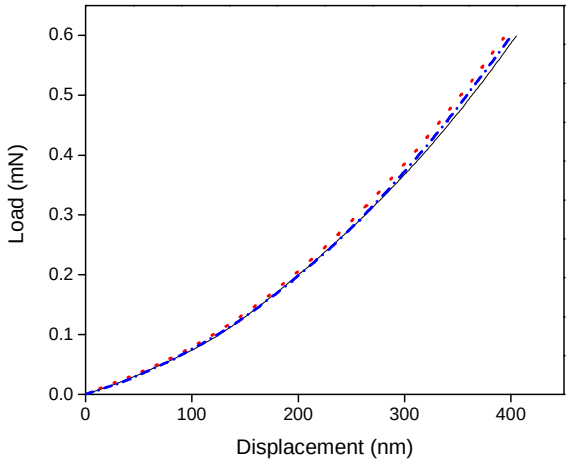

A.4 Load-displacement curves of PVAc obtained using Triboindenter at 32.1 ^{o}C

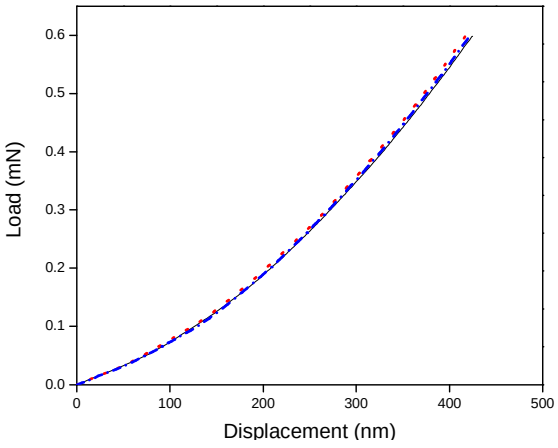

A.5 Load-displacement curves of PVAc obtained using Triboindenter at 34.1 ^{o}C

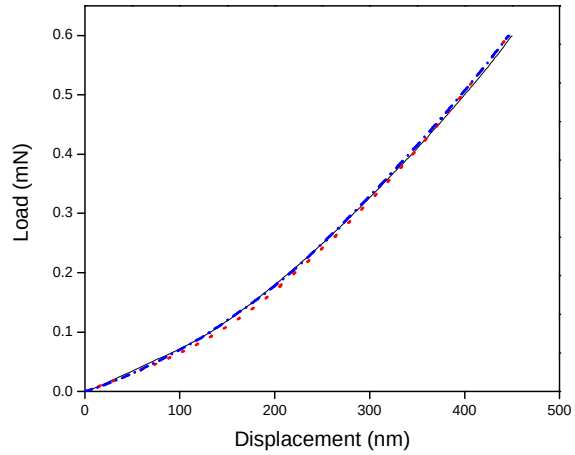

A.6 Load-displacement curves of PVAc obtained using Triboindenter at 36.6 ^{o}C

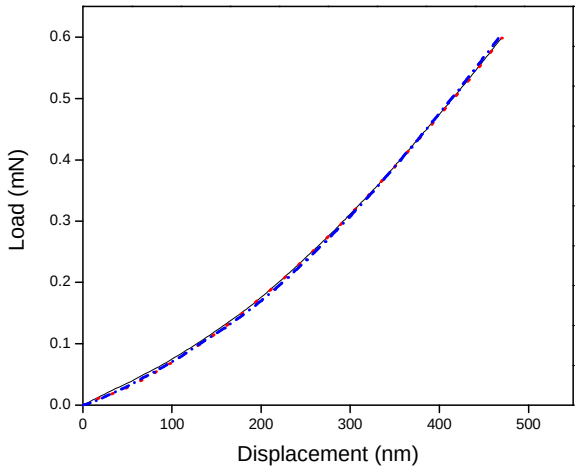

A.7 Load-displacement curves of PVAc obtained using Triboindenter at 38 ^{o}C

VITA

Dilek Cakiroglu

Candidate for the Degree of

Master of Science

Thesis: AN EXPLORATORY INVESTIGATION OF VISCOELASTIC NANOINDENTATION ON POLYVINYL ACETATE

Major Field: Mechanical Engineering

Biographical:

Education:
Completed Bachelor of Science degree in Engineering Physics and Master of Science degree in Polymer Science at Istanbul Technical University. Completed the requirements for the Master of Science in Mechanical Engineering at Oklahoma State University, Stillwater, Oklahoma in May, 2009.

Experience:
Graduate Research Assistant, Mechanical Engineering, OSU
Mathematic Tutor, University Academic Service, OSU
Graduate Research Assistant, Polymer Science and Technology, ITU
Graduate Teaching Assistant, Engineering Physics, ITU

Name: Dilek Cakiroglu Date of Degree: May, 2009

Institution: Oklahoma State University Location: Stillwater, Oklahoma

Title of Study: AN EXPLORATORY INVESTIGATION OF VISCOELASTIC NANOINDENTATION ON POLYVINYL ACETATE

Pages in Study: 36 Candidate for the Degree of Master of Science

Major Field: Mechanical Engineering

Scope and Method of Study: Nanoindentation load-displacement data of polyvinyl acetate (PVAc) was obtained at different temperatures ranging from ~20 ^{o}C to 42 ^{o}C using two novel equipments, Hysitron Triboindenter and Interfacial Force Microscopy (IFM). Load-displacement data was analyzed using viscoelastic contact theory and JKR contact mechanics theory.

Findings and Conclusions: Load-displacement data obtained by Hysitron Triboindenter was analyzed using viscoelastic theory and shear creep compliance curves were obtained at different temperatures. Load-displacement data obtained by IFM was analyzed using viscoelastic theory and JKR contact mechanics theory and shear creep compliance curves were obtained at different temperatures. Small drift rate in load-displacement data obtained by Hysitron Triboindenter resulted in big error in shear creep compliance curves so that master shear creep compliance curve could not be formed. Glass transition temperature of PVAc was found at ~34 ^{o}C using shear creep compliance curves and it showed that glass transition temperature of PVAc is not unique. Adhesion forces between PVAc and tip was observed by IFM and invalidity of JKR method for PVAc was shown.

ADVISER'S APPROVAL: Dr. Hongbing Lu